SUPPORTING INFORMATION

A Chemical Biological Strategy to Facilitate Diabetic Wound Healing

Major Gooyit,[†] Zhihong Peng,[†] William R. Wolter,[‡] Hualiang Pi,[†] Derong Ding,[†] Dusan Hesek,[†] Mijoon Lee,[†] Bill Boggess,[†] Matthew M. Champion,[†] Mark A. Suckow,[‡] Shahriar Mobashery,[*, †] and Mayland Chang[*, †]

[†]Department of Chemistry and Biochemistry, University of Notre Dame, Notre Dame, IN 46556, USA

[‡]Freimann Life Sciences Center and Department of Biological Sciences, University of Notre Dame, Notre Dame, IN 46556, USA

Animals. Female diabetic *db/db* (n = 94, BKS.Cg-*Dock7^m* +/+ *Lepr^{db}*/J, 6-8 weeks, 38-40 g) and wild-type mice (n = 70, C57BLKS/6J, 6-8 weeks, 18-20 g, same background as diabetic mice; Jackson Laboratory) were used. All procedures were performed in accordance with the University of Notre Dame Institutional Animal Care and Use Committee. Mice were provided with Laboratory 5001 Rodent Diet (PMI) and water *ad libitum*, and maintained in polycarbonate shoebox cages with hardwood bedding at 72 ± 2 °F and a 12:12 h light/dark cycle.

Excisional Diabetic Wound Model. Single excisional 8-mm diameter wounds were made with a biopsy punch (Miltex) using aseptic technique in the shaved dorsal regions under isoflurane anesthesia.[1] For the evaluation of ND-322 on wound healing, wild-type and *db/db* mice were each divided into two groups (35 per group): ND-322 (50 μL of 5.0 mg mL^{-1}, equivalent to 0.25 mg per wound) and vehicle (50 μL saline). Wounds were photographed and immediately covered with a sterile dressing (3M Tegaderm™ Transparent Dressing, Butler Schein Animal Health, Inc.). Cellulose acetate collars were made in-house and mounted on the wild-type mice to prevent them from disturbing the wounds.[2] In our experience, wild-type mice typically remove the dressing and chew at the wound sites, while diabetic mice are not able to reach the wound sites, because of obesity. Topical treatment with ND-322 or vehicle (saline) commenced one day after wounding and continued for 14 days. On days 1, 3, 7, 10, and 14, digital photographs of wounds were taken while animals were under isoflurane anesthesia. On the same days, 14 mice (n = 7 for each ND-322 and vehicle) were sacrificed. The wounds with minimal surrounding healthy tissue were excised and either flash-frozen in liquid nitrogen for protein expression profiling or embedded in optimal cutting temperature (OCT) compound (Tissue-Tek), followed by cryosectioning for histological assessment. For the evaluation of MMP-8 inhibitor on wound healing in diabetic mice, the same procedure, as detailed above, was performed. Diabetic mice were each divided into two groups (12 per group): MMP-8 inhibitor (50 μL of 5.0 mg mL^{-1}, equivalent to 0.25 mg per wound) and vehicle (50 μL of 80% propylene glycol/20% DMSO). Digital photographs of wounds were taken on days 0, 7, 10, and 14 while animals were under isoflurane anesthesia. On days 7 and 14, 12 mice (n = 6 for each MMP-8 inhibitor and vehicle) were sacrificed. The wounds were excised, embedded in OCT, and cryosectioned for histological evaluation.

Photographs were taken using a digital camera (Olympus SP-800UZ) statically mounted on a tripod at a fixed distance above the wound; a ruler was included in the photographic frame. The digital images were analyzed with NIH ImageJ version 1.45 software. The wound outline was defined from the photographic image and the ImageJ software calculated the wound area. Wound healing was expressed as the change in wound area relative to that from day 0.

MMP-Expression Profiling. A 2-μL aliquot of the ZipTip® cleaned peptide mixtures were then analyzed on a reversed phase Waters nanoACQUITY column (1.7 μm, BEH130 C18, 100 μm i.d. x 100 μm, Waters Corp.) coupled to a Thermo LTQ Velos Orbitrap tandem mass spectrometer (Thermo Fisher Scientific). Samples were eluted at 1.2 μL min^{-1} t = 0-5 min 99%A/1%B, t = 5.1 min 85%A/15%B, t = 50 min 40%A/60%B, t = 55 min 15%A/85%B, t = 55.1-65 min 99%A/1%B where A = 97% water/3% acetonitrile/ 0.1% formic acid and B = 0.1% formic acid in acetonitrile. Peptides were ionized via a nanoelectrospray ionization (ESI) source, and their mass spectra and collisionally induced dissociation (CID) fragmentation mass spectra were recorded. High resolution (60,000 resolving power), accurate mass spectra were recorded between *m/z* 395-2,000 in ~1.2 sec on the orbitrap mass analyzer. While the next high-resolution mass spectrum was being acquired on the orbitrap, the LTQ Velos linear ion trap independently recorded CID fragmentation mass spectra of the 8 most abun-

dant ions present in the previous orbitrap mass spectrum. During the course of a 60-min nanoUPLC/MS/MS run, this approach typically generated ~3,000 high-resolution mass spectra and between 12,000-15,000 CID MS/MS spectra.

Thermo-Finnegan Proteome Discoverer 2.0 software (Thermo Fisher Scientific) was used to interface with the Mascot (Matrix Science) protein database search engine. MS/MS spectral information was used by Mascot to search the SwissProt Protein database, and a decoy search was employed to establish a false discovery rate. Standard solutions of MMPs that had been digested and analyzed using the approach described herein then served as references by which all results from the tissue-derived samples would be directly compared.

Zymography. Aliquots of the tissue extracts (0.4 mg protein) were subjected to affinity precipitation with gelatin-agarose beads. The bound gelatinases were released from the beads in 2% SDS, and the samples were analyzed by electrophoresis in a 10% gelatin zymogram gel, as previously described.[3]
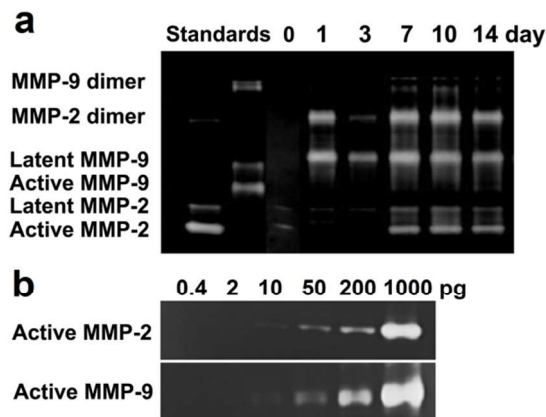

Figure 1 (a) Gelatin zymography of wound tissue extracts from *db/db* mice; proMMP-2, proMMP-9, and active MMP-2 are observed, however active MMP-9 is not detectable for lack of sensitivity. The faint band below MMP-9 dimer on days 7, 10, and 14 is likely the previously reported complex between MMP-8 and MMP-9.[4] Since active MMP-2 is not detected with the resin method, the active MMP-2 band seen by gelatin zymography represents the TIMP-inhibited MMP-2, a non-covalent complex. The SDS used in gelatin zymography denatures the TIMP-MMP complex, appearing as an active MMP-2 band. Thus, detection of inactive TIMP-inhibited gelatinases as active bands is a major drawback of gelatin zymography. (b) Sensitivity of MMP-2 and MMP-9 by gelatin zymography; the limit of detection of MMP-2 and MMP-9 is 10 pg.

Histological Evaluation, *In-situ* Zymography and Apoptosis Detection. Fresh wound tissue was cut, embedded in OCT compound, and cryosectioned at a thickness of 12-μm for hematoxylin-eosin (H&E) staining, and at 8-μm for *in-situ* zymography and apoptosis detection. Morphological assessment of re-epithelialization was performed on a Nikon Eclipse 90*i* Fluorescent Microscope (Nikon Instruments Inc.).[5] The procedure for *in-situ* zymography was adapted from Oh *et al.*[6] Evaluation of apoptosis was performed using DermaTACS[TM] Apoptosis detection kit (Trevigen Inc.), following the manufacturer's instructions.

Quantification of MMPs in Wound Tissues. Following trypsin digestion, samples were desalted using Millipore ZipTip® C18 (EMD Millipore Corp.), according to the manufacturer's instructions. Briefly, each ZipTip® was wetted with HPLC-grade acetonitrile, equilibrated with 0.1% trifluoroacetic acid (TFA) in HPLC-grade water, loaded with 4 μL of digested sample, washed with 0.1% TFA in water, and eluted with 0.1% TFA in 50:50 (v:v) acetonitrile:water. This procedure was repeated until ~20 μL of the eluted solution had been collected in an autosampler vial. The ZipTip® samples were concentrated to dryness on a miVac concentrator (Genevac Ltd.) and the residue was resuspended (12 μL water containing 1% formic acid) and internal standard (yeast enolase at a final concentration of 150 fmol mg^{-1} tissue) was added. A 2-μL aliquot was injected directly onto a nanoACQUITY UPLC C18 column (1.8 μm, 100 μm i.d. ×100 mm, Waters Corp.) and eluted at 600 nL min^{-1} with 2% acetonitrile/0.1% formic acid/water for 12 min, followed by a 60-min linear gradient to 35% acetonitrile/0.1% formic acid/water. Samples were analyzed on a ABSciex QTrap 5500 mass spectrometer (ABSciex) running in ion trap IDA mode coupled to a two-dimensional Eksignet Ultra NanoUPLC system, consisting of a nanoLC ultra 2D pump and a nanoLC AS-2 autosampler (Eksignet). The mass spectrometer was operated in the positive ESI mode: curtain gas 20 psi, ion spray voltage 2350 V, ion source gas 1 10 psi, declustering potential 100V, entrance potential 10V, collision cell exit potential 40V. Acquisition parameters were as described previously.[7]

MRM transitions were determined through the use of empirical MS/MS data obtained from the bottom-up proteomics analysis and through the use of *in silico* prediction, as described previously.[7] MMP-8 and MMP-9 were quantified using three product-ion transitions per peptide, with one as the 'quantifier' and two as the 'qualifier' transitions (Table 1). The quantifier MMP-8 specific tryptic peptide **[CAm]**CGVPDSGDFLLTPGSPK was observed and quantified for the transition m/z 873.92 $(M+2H)^{2+}$ → product ion m/z 935.36 $(M+H)^+$ corresponding to the b10 ion. The MMP-9 specific tryptic peptide AFAVWGEVAPLTFTR observed at m/z 832.94 $(M+2H)^{2+}$ → product ion m/z 1033.57 $(M+H)^+$ (y9) was used. Quantification of MMP-8 and MMP-9 was relative to the yeast enolase (internal standard) peptide NVNDVIAPAFV**K** at m/z 643.86 $(M+2H)^{2+}$ → product ion m/z 632.38 $(M+H)^+$ (y6). Standard calibration curves of MMP-8 and MMP-9 were prepared in control mouse skin tissue at concentrations of 0.6, 6.0, 15, 30, 60, 150, 300, and 600 fmol mg^{-1} tissue. Concentrations in unknown samples were determined using peak area ratios relative to the internal standard and calibration curve regression parameters.

Characterization of Compound 3. Compound **3**, synthesized by the literature method, had identical spectroscopic data to that reported in the literature.[8] Purity was >99%.
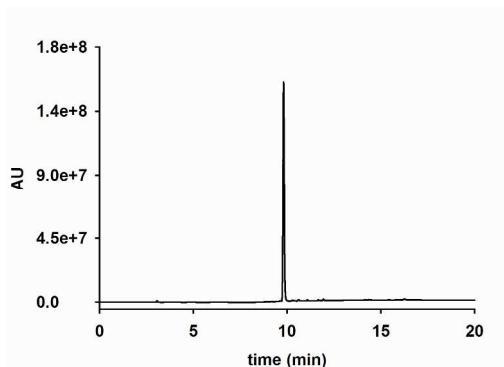

Figure 2 HPLC chromatogram of compound **3**. Conditions: Zorbax RX-C8 5μm, 4.6 mm i.d. x 250 mm (Agilent), 0.7 mL min^{-1}, 30% acetonitrile/70% water for 4 min, 8-min linear gradient to 90% acetonitrile/10% water, 6-min 90% acetonitrile/10% water, UV detection at 285 nm.

Table 1 Peptides and internal standard selected for MRM

Protein	Peptide Sequence	Q1 Precursor Ion m/z	Q3 Product Ions m/z
MMP-8	**[Cam]**CGVPDSGDFLLTPGSP**K**	873.92 [M+2H]$^{2+}$	935.36 [M+H]$^+$ b10, 1074.58 [M+H]$^+$ y10, 959.56 [M+H]$^+$ y9
MMP-9	AFAVWGEVAPLTFT**R**	832.94 [M+2H]$^{2+}$	1090.59 [M+H]$^+$ y10, 1033.57 [M+H]$^+$ y9, 734.42 [M+H]$^+$ y6
		555.63 [M+3H]$^{3+}$	1090.59 [M+H]$^+$ y10, 1033.57 [M+H]$^+$ y9, 734.42 [M+H]$^+$ y6
Yeast enolase	NVNDVIAPAFV**K**	643.86 [M+2H]$^{2+}$	632.38 [M+H]$^+$ y6, 844.53 [M+H]$^+$ y8, 561.34 [M+H]$^+$ y5

Cam = carbamidomethylated; yeast enolase was used as internal standard

Blood Collection and Sample Analysis. Blood samples were collected from diabetic mice in heparinized syringes through the posterior vena cava on day 7 at 30 min after topical administration of ND-322 or MMP-8 inhibitor **3** at 0.25 mg per wound per day. Blood samples were stored on ice and centrifuged to collect plasma. A 50-μL aliquot of plasma was mixed with 100-μL of internal standard **4** in acetonitrile to a final concentration of 1 μM. The supernatants were analyzed by reversed-phase UPLC/(+)-ESI-MRM of the transitions 322→185 for ND-322, 468→162 for MMP-8 inhibitor **3**, and 300→93 for internal standard **4**. The internal standard was synthesized as previously described.[8] Calibration curves of ND-322 and MMP-8 inhibitor **3** were prepared by fortification of blank mouse plasma with ND-322 and compound **3** at concentrations up to 2 μM. Quantification was performed using peak area ratios relative to the internal standard **4** and linear regression parameters calculated from the calibration curve standards.

Plasma levels of ND-322 were 130 ± 88 nM at 30 min on day 7 after multiple-dose topical administration. These concentrations were significantly below the K_i for MMP-9 of 870 nM, whereas levels of MMP-8 inhibitor **3** (81 ± 50 nM at 30 min on day 7) were above the K_i for MMP-8 of 25 nM. Our results showed that ND-322 was efficacious within the diabetic wound when applied topically and that it did not reach high enough systemic concentrations to manifest activity elsewhere in the body. This is a desired attribute for ND-322 as a potential topical treatment for diabetic wound healing.

4
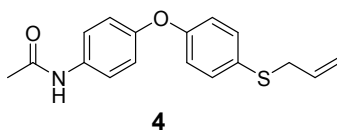
Liquid Chromatography/Mass Spectrometry. The LC system consisted of a Waters Acquity UPLC (Waters Corporation) equipped with a binary solvent manager, an autosampler, a column heater, and a photodiode array detector. The MRM-MS experiments were conducted using a Waters TQD tandem quadrupole detector (Milford) with MassLynx MS software. The following conditions were used: capillary voltage 2.8 kV, cone voltage 35 V, extractor voltage 3 V, RF lens voltage 0.3 V, desolvation nitrogen gas flow rate 650 L hr^{-1}, cone nitrogen gas flow rate 20 L h^{-1}, source temperature 150 ^{o}C, and desolvation temperature 350 ^{o}C. Samples were analyzed on an Acclaim RSLC

120 C18 column (2.2 μm, 2.1 mm i.d. × 100 mm, Dionex). The mobile phase consisted of elution at 0.5 mL min^{-1} with 85% A/15% B for 1 min, followed by a 6-min linear gradient to 10% A/90% B and then 10% A/90% B for 2 min (A = 0.1% formic acid in water; B = 0.1% formic acid in acetonitrile).

Statistical Analyses. Data are expressed as mean ± SD (For levels of MMP-8 and MMP-9: n = 3. For evaluation of ND-322 on wound healing: n = 35 on day 1; n = 28 on day 3; n = 21 on day 7; n = 14 on day 10; n = 7 on day 14. For evaluation of MMP-8 inhibitor **3** on wound healing in diabetic mice: n = 12 on day 7; n = 6 on day 10; n = 6 on day 14. For levels of ND-322 and MMP-8 inhibitor **3** in plasma: n = 3). Wound healing and levels of MMP-8 and MMP-9 were analyzed for statistical significance using a paired Student t-test; $p <$ 0.05 was considered statistically significant.

REFERENCES

(1) Sullivan, S. R., Underwood, R. A., Gibran, N. S., Sigle, R. O., Usui, M. L., Carter, W. G., and Olerud, J. E. (2004) Validation of a model for the study of multiple wounds in the diabetic mouse (db/db), *Plast Reconstr Surg 113*, 953-960.

(2) Einheber, A., Wren, R. E., Carter, D., and Rose, L. R. (1967) A simple collar device for the protection of skin grafts in mice, *Lab Anim Care 17*, 345-348.

(3) Toth, M., and Fridman, R. (2001) Assessment of Gelatinases (MMP-2 and MMP-9) by Gelatin Zymography, *Methods Mol Med 57*, 163-174.

(4) Gutierrez-Fernandez, A., Inada, M., Balbin, M., Fueyo, A., Pitiot, A. S., Astudillo, A., Hirose, K., Hirata, M., Shapiro, S. D., Noel, A., Werb, Z., Krane, S. M., Lopez-Otin, C., and Puente, X. S. (2007) Increased inflammation delays wound healing in mice deficient in collagenase-2 (MMP-8), *FASEB J 21*, 2580-2591.

(5) Tkalcevic, V. I., Cuzic, S., Parnham, M. J., Pasalic, I., and Brajsa, K. (2009) Differential evaluation of excisional non-occluded wound healing in db/db mice, *Toxicol Pathol 37*, 183-192.

(6) Oh, L. Y., Larsen, P. H., Krekoski, C. A., Edwards, D. R., Donovan, F., Werb, Z., and Yong, V. W. (1999) Matrix metalloproteinase-9/gelatinase B is required for process outgrowth by oligodendrocytes, *J Neurosci 19*, 8464-8475.

(7) Llarrull, L. I., Toth, M., Champion, M. M., and Mobashery, S. (2011) Activation of BlaR1 protein of methicillin-resistant Staphylococcus aureus, its proteolytic processing, and recovery from induction of resistance, *J Biol Chem 286*, 38148-38158.

(8) Ikejiri, M., Bernardo, M. M., Bonfil, R. D., Toth, M., Chang, M., Fridman, R., and Mobashery, S. (2005) Potent mechanism-based inhibitors for matrix metalloproteinases, *J Biol Chem 280*, 33992-34002.